

Manipulator velocity control using friction compensation

J. Moreno, R. Kelly and R. Campa

Abstract: The velocity control of a direct-drive mechanical arm with high friction is considered. The friction at the robot joints is assumed to be captured by a bristle deflection model. Two joint velocity controllers with friction compensation are introduced. Experiments show the superiority of the proposed schemes with respect to the velocity controllers when friction is compensated using the classical viscous plus Coulomb model of friction.

1 Introduction

Friction is a phenomenon that deteriorates the good motion performance of servomechanisms, such as robots and machine tools. Model-oriented friction compensation techniques are based on the knowledge of a suitable friction model that predicts the real friction and commands an opposed control action to compensate it [1].

Velocity control of mechanical systems is a well studied subject in the literature. In the seminal paper reported by Canudas de Wit *et al.* [2], theorem 2 is concerned with a velocity observer-based controller utilising the LuGre friction model. Asymptotic stability of such a controller was later established in [3]. In [4] a velocity controller was proposed based on a modified Coulomb friction model. In the work reported by [5] experimental results on velocity control were shown using a friction estimation and compensation technique based on a Coulomb friction observer.

Velocity control is also an important theoretical and practical issue in robotic manipulators. The concept of kinematic control [6] deals with the end-effector posture, position and orientation, control under the assumption that the robot joint velocities are the manipulator's inputs. This assumption may hold only when suitable velocity controllers are incorporated in each robot joint. The actual situation in many industrial robots is that the control of each axis is carried out making use of an inner velocity loop in addition to an outer position loop [7, 8]. These velocity loops arise from individual velocity regulators of the corresponding electrical motors where feedforward compensation is added to handle disturbances due to manipulator nonlinear dynamics [9].

Dynamic friction models, such as the Dahl model [10] and LuGre model [2], are able to predict important phenomena that appear at low velocities such as presliding displacement. The Dahl model describes, in a simple

fashion, the spring-like behaviour during stiction [2]. Let us note that the Dahl model is essentially Coulomb friction with a lag in the change of friction force when the direction of motion is changed [1]. Thus, we have found that the Dahl model of friction closely matches with experiments carried out in our direct-drive actuators. Fig. 1 depicts the experimental velocity response as well as a simulation using the Dahl model for a Compumotor's DM1004C direct-drive motor with a torque ramp input $\tau(t) = 0.5t$. This experimental evidence has prompted us to carry out a study on friction compensation techniques based on the Dahl model.

We present a study on joint velocity control in manipulators using compensation of friction. Two controllers based in the Dahl model are proposed and their performance is compared with respect to friction compensation based on the classical static model of viscous and Coulomb friction. The discussed experimental evaluation of the velocity controllers has been conducted on a two degrees-of-freedom direct-drive arm. Direct-drive robots, those robots without transmission mechanisms from the motor shaft to links, offer the interesting challenge of their nonlinear dynamics. Advantages of such a class of manipulators are the absence of backlash and high stiffness, all of which represents profit for applications in fast and accurate motions [11].

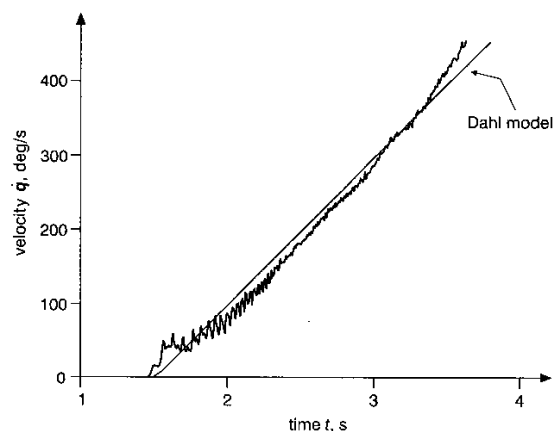


Fig. 1 Velocity responses

© IEE, 2003

IEE Proceedings online no. 20030083

DOI: 10.1049/ip-cta:20030083

Paper first received 21st March 2002

The authors are with the División de Física Aplicada, CICESE, Apdo. Postal 2615, Adm. 1, Ensenada, B.C., 22800, Mexico

The following notation will be adopted. $\|x\| = \sqrt{x^T x}$ stands for the norm of vector $x \in \mathbb{R}^n$. $\lambda_{\min}\{A(x)\}$ and $\lambda_{\max}\{A(x)\}$ denote the minimum and maximum eigenvalues of a symmetric positive definite matrix $A(x) \in \mathbb{R}^{n \times n}$ for all $x \in \mathbb{R}^n$, respectively. $\sqrt{\lambda_{\max}\{B(x)^T B(x)\}}$ stands for the induced norm of a matrix $B(x) \in \mathbb{R}^{n \times n}$ for all $x \in \mathbb{R}^n$.

2 Robot model and control aim

The dynamics in joint space of a serial-chain n -link robot manipulator considering the presence of friction at the joints can be written as:

$$M(q)\ddot{q} + C(q, \dot{q})\dot{q} + g(q) + f(z, \dot{q}) = \tau \quad (1)$$

where q is the $n \times 1$ vector of joint displacements, \dot{q} is the $n \times 1$ vector of joint velocities, τ is the $n \times 1$ vector of applied torque inputs, $M(q)$ is the $n \times n$ symmetric positive definite manipulator inertia matrix, $C(q, \dot{q})\dot{q}$ is the $n \times 1$ vector of centripetal and Coriolis torques, $g(q)$ is the $n \times 1$ vector of gravitational torques, and $f(z, \dot{q})$ is the $n \times 1$ vector of torques due to the friction which depends on the joint velocity $\dot{q} \in \mathbb{R}^n$ and an unmeasurable internal state $z \in \mathbb{R}^n$ which will be defined below.

One of the simplest dynamic models, inspired on a bristle deflection interpretation, is that due to Dahl [10] which, including viscous friction, can be described by:

$$\dot{z} = -\Psi(\dot{q})z + \dot{q} \quad (2)$$

$$f(z, \dot{q}) = \Sigma_0 z + F_v \dot{q} \quad (3)$$

where $F_v = \text{diag}\{f_{v_1}, \dots, f_{v_n}\}$ is a diagonal positive definite matrix which contains the viscous friction coefficient of each joint, $\Sigma_0 = \text{diag}\{\sigma_0, \dots, \sigma_0\}$ is a diagonal positive definite matrix which contains the 'stiffness' parameter of each joint, and

$$\Psi(\dot{q}) = \text{diag}\left\{\frac{\sigma_0}{f_{c_1}}|\dot{q}_1|, \dots, \frac{\sigma_0}{f_{c_n}}|\dot{q}_n|\right\}$$

is a diagonal positive semidefinite matrix where f_{c_i} denotes the Coulomb parameter for each joint $i = 1, \dots, n$. It can be shown that this friction model satisfies the requirements stated in [12] to get a passive operator from velocity \dot{q} to friction force f .

Assuming that the desired joint velocity specification $\omega_d(t)$ is continuously differentiable, bounded by $\|\omega_d\|_M$ i.e.:

$$\|\omega_d(t)\| \leq \|\omega_d\|_M \quad \forall t \geq 0$$

and knowledge of parameters of the robot model (1), (2), and (3), thus the control objective is to achieve

$$\lim_{t \rightarrow \infty} \tilde{\omega}(t) = \theta \quad (4)$$

where $\tilde{\omega} = \omega_d - \dot{q}$ denotes the joint velocity error.

3 Velocity control

Two velocity control algorithms are introduced in this Section. The first controller is motivated by an inverse dynamics structure and uses a Dahl-based exponentially convergent observer, while the second one is based in a proportional and derivative (PD) control with compensation structure. A Dahl-based stable observer is proposed for the PD control with compensation. The use of a static model of viscous and Coulomb friction for compensation in velocity control is also discussed in this Section.

3.1 Inverse dynamics controller

Consider the following controller which is inspired from the inverse dynamics technique [6]:

$$\tau = M(q)[\dot{\omega}_d + K_v \tilde{\omega} + K_i \xi] + C(q, \dot{q})\dot{q} + g(q) + F_v \dot{q} + \Sigma_0 \hat{z} \quad (5)$$

$$\dot{\xi} = \tilde{\omega} \quad (6)$$

where K_i and K_v are $n \times n$ symmetric positive definite matrices, and \hat{z} is an estimation of the unmeasurable state z of the Dahl friction model (2) and (3).

We propose the following observer for the z state:

$$\dot{x} = -\Psi(\dot{q})[x + K_0 \tilde{\omega}] + \dot{q} + K_0[K_v \tilde{\omega} + K_i \xi] \quad (7)$$

$$\hat{z} = x + K_0 \tilde{\omega} \quad (8)$$

where $K_0 = \text{diag}\{k_{01}, \dots, k_{0n}\}$ is a diagonal positive definite matrix. Fig. 2 shows a block diagram of implementation of controller (5) and (6), and observer (7) and (8).

Substituting the controller (5) and (6) into the robot dynamics (1) we obtain:

$$\dot{\tilde{\omega}} + K_v \tilde{\omega} + K_i \xi + M(q)^{-1} \Sigma_0 \tilde{z} = \theta \quad (9)$$

where

$$\tilde{z} = \hat{z} - z \quad (10)$$

denotes the observation error of the internal state z .

Differentiating (8) with respect to time and substituting into (7), it is possible to obtain the expression given by:

$$\dot{\hat{z}} = -\Psi(\dot{q})\hat{z} + \dot{q} - K_0 M(q)^{-1} \Sigma_0 \tilde{z} \quad (11)$$

Using (3), (6), (9), (10), and (11) we can write the closed-loop system as follows

$$\frac{d}{dt} \begin{bmatrix} \xi \\ \tilde{\omega} \\ \tilde{z} \end{bmatrix} = \begin{bmatrix} \tilde{\omega} \\ -K_v \tilde{\omega} - K_i \xi - M(q)^{-1} \Sigma_0 \tilde{z} \\ -\Psi(\omega_d - \tilde{\omega})\tilde{z} - K_0 M(q)^{-1} \Sigma_0 \tilde{z} \end{bmatrix} \quad (12)$$

System (12) has an equilibrium point at the origin of the state space.

In order to prove that the equilibrium of system (12) is globally asymptotically stable we propose the following Lyapunov function

$$V(\xi, \tilde{\omega}, \tilde{z}) = \frac{1}{2} \tilde{\omega}^T \tilde{\omega} + \frac{1}{2} \xi^T K_i \xi + \frac{\alpha}{2} \tilde{z}^T \Sigma_0 K_0^{-1} \tilde{z} \quad (13)$$

where α is a constant large enough in the sense

$$\alpha > \frac{\lambda_{\max}\{\Sigma_0 M(q)^{-1} M(q)^{-1} \Sigma_0\}}{4 \lambda_{\min}\{K_v\} \lambda_{\min}\{\Sigma_0 M(q)^{-1} \Sigma_0\}} \quad (14)$$

The time derivative of (13) along the system trajectories (12) is given by

$$\begin{aligned} \dot{V}(\xi, \tilde{\omega}, \tilde{z}) &= -\tilde{\omega}^T K_v \tilde{\omega} - \alpha \tilde{z}^T \Sigma_0 K_0^{-1} \Psi(\dot{q}) \tilde{z} \\ &\quad - \alpha \tilde{z}^T \Sigma_0 M(q)^{-1} \Sigma_0 \tilde{z} - \tilde{\omega}^T M(q)^{-1} \Sigma_0 \tilde{z} \end{aligned}$$

Using the property that $M(q)^{-1}$ is a symmetric positive definite matrix, see e.g. Canudas de Wit *et al.* [6], it is possible to obtain an upper bound on $\dot{V}(\xi, \tilde{\omega}, \tilde{z})$ as follows

$$\dot{V}(\xi, \tilde{\omega}, \tilde{z}) \leq W(\xi, \tilde{\omega}, \tilde{z})$$

where

$$W(\xi, \tilde{\omega}, \tilde{z}) = - \begin{bmatrix} \|\tilde{\omega}\| \\ \|\tilde{z}\| \end{bmatrix}^T Q \begin{bmatrix} \|\tilde{\omega}\| \\ \|\tilde{z}\| \end{bmatrix} \quad (15)$$

The PD control with compensation-based controller with friction compensation using the static model (25) is:

$$\tau = M(q)[\dot{\omega}_d + \Lambda \tilde{\omega}] + C(q, \dot{q})[\omega_d + \Lambda \tilde{\xi}] + g(q) + K_v \tilde{\omega} + K_i \tilde{\xi} + F_v \dot{q} + F_C \text{sign}(\dot{q}) \quad (28)$$

$$\dot{\tilde{\xi}} = \tilde{\omega} \quad (29)$$

4 Experimental results

We have built at CICESE Research Centre a two degrees-of-freedom experimental direct-drive robot arm to enable real-time control experiments. The arm moves in the vertical plane as shown in Fig. 4. The motors used in the robot arm are the DM1015-B and DM1004-C models from Parker Compumotor for the shoulder and elbow joints respectively. The motors are operated in torque mode, so they act as a torque source and accept an analog voltage as a reference torque signal. The control algorithm is executed at 1 ms sampling period in a PC host computer equipped with the MFIO-3A data acquisition board from Precision MicroDynamics.

We now present the entries of the robot dynamics. The elements $M_{ij}(q)$ ($i, j = 1, 2$) of the inertia matrix are:

$$M_{11}(q) = 0.3353 + 0.02436\cos(q_2)$$

$$M_{12}(q) = 0.01267 + 0.01218\cos(q_2)$$

$$M_{21}(q) = 0.01267 + 0.01218\cos(q_2)$$

$$M_{22}(q) = 0.01267$$

The elements $C_{ij}(q, \dot{q})$ ($i, j = 1, 2$) of the centrifugal and Coriolis matrix are:

$$C_{11}(q, \dot{q}) = -0.01218\sin(q_2)\dot{q}_2$$

$$C_{12}(q, \dot{q}) = -0.01218\sin(q_2)\dot{q}_1 - 0.01218\sin(q_2)\dot{q}_2$$

$$C_{21}(q, \dot{q}) = 0.01218\sin(q_2)\dot{q}_1$$

$$C_{22}(q, \dot{q}) = 0.0$$

The entries of the gravitational torque vector $g(q)$ are given by:

$$g_1(q) = g[1.1731\sin(q_1) + 0.04685\sin(q_1 + q_2)]$$

$$g_2(q) = g[0.04685\sin(q_1 + q_2)]$$

where $g = 9.81 \text{ m/s}^2$.

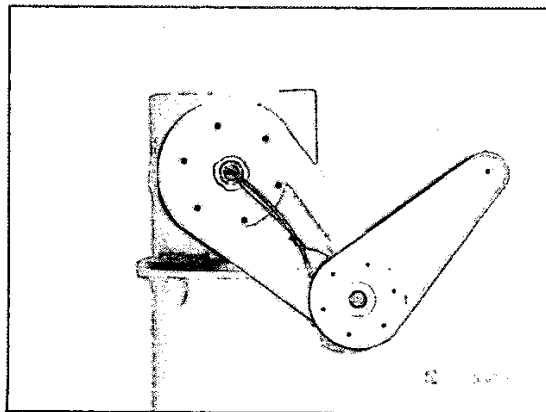


Fig. 4 Experimental arm

Following the procedures of [16, 17], and references therein, we have estimated the parameters of the Dahl model of friction for the experimental arm. For joint 1:

$$\sigma_{01} = 1757 \text{ Nm/rad}$$

$$f_{C1} = 1.29 \text{ Nm}$$

$$f_{v1} = 0.2741 \text{ Nm s/rad}$$

For joint 2:

$$\sigma_{02} = 2764 \text{ Nm/rad}$$

$$f_{C2} = 0.965 \text{ Nm}$$

$$f_{v2} = 0.1713 \text{ Nm s/rad}$$

Joint velocity control experiments have been carried out in order to compare the performance of the Dahl-based velocity controllers with respect to the velocity controllers that use the static model of viscous and Coulomb friction for compensation. The specified desired velocity ω_d is given by:

$$\omega_{d1} = 4.7124t^2 e^{-2t^3} + 4.2t^2 e^{-2t^3} \sin(6t) + 4.2[1 - e^{-2t^3}] \cos(6t) \text{ (rad/s)}$$

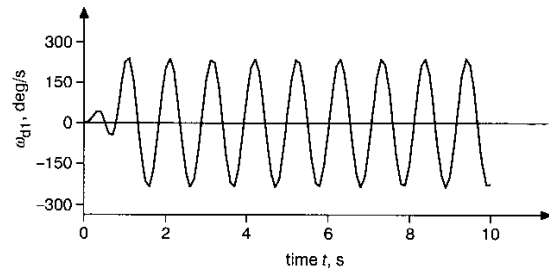
$$\omega_{d2} = 6.2832t^2 e^{-2t^3} + 7.0896t^2 e^{-2t^3} \sin(3t) + 3.5448[1 - e^{-2t^3}] \cos(3t) \text{ (rad/s)}$$

Fig. 5 shows the time evolution of $\omega_{d1}(t)$ and $\omega_{d2}(t)$. It should be noticed that at $t=0$ the desired velocity ω_d as well as the desired acceleration $\dot{\omega}_d$ are zero.

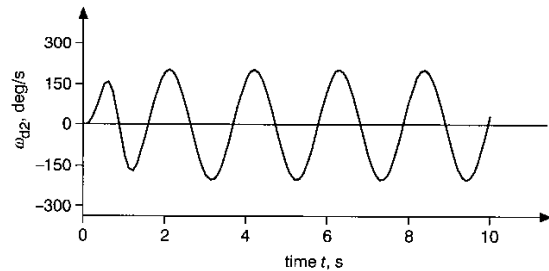
The inverse-dynamics-based controllers (5) and (6), and (26) and (27), were implemented with gains:

$$K_i = \text{diag}\{900, 900\} \text{ (1/s}^2\text{)}$$

$$K_v = \text{diag}\{60, 60\} \text{ (1/s)}$$



a



b

Fig. 5 Desired velocity

a ω_{d1} against time

b ω_{d2} against time

The observer (7) and (8) was applied using $K_0 = \text{diag}\{0.0045, 0.0045\}$ (s). On the other hand, experiments with the PD with compensation-based controllers (17) and (18), and (28) and (29) were tested using:

$$K_i = \text{diag}\{10, 5\} \text{ (Nm/rad)}$$

$$K_v = \text{diag}\{5, 4\} \text{ (Nm s/rad)}$$

$$\Lambda = K_v^{-1} K_i = \text{diag}\{2, 1.25\} \text{ (s}^{-1}\text{)}$$

4.1 Inverse dynamics controller

Fig. 6 shows the velocity error using the velocity controller (26) and (27), which considers viscous and Coulomb friction compensation. On the other hand, Fig. 7 depicts the velocity error using the Dahl-based velocity controller (5)–(8). Using controller (26) and (27), the maximum peak error is 5.55° 1/s and 42.2° 1/s for $\tilde{\omega}_1$, and $\tilde{\omega}_2$, respectively; while using the Dahl-based controller (5)–(8) the maximum peak error is 5.12° 1/s and 27.24° 1/s for $\tilde{\omega}_1$, and $\tilde{\omega}_2$, respectively. The Dahl-based controller (5)–(8) has a better performance than controller (26) and (27), which considers only viscous and Coulomb friction compensation. The improvement can be computed as 7.75% for $\tilde{\omega}_1$ and 35.45% for $\tilde{\omega}_2$.

4.2 PD control with compensation

Fig. 8 depicts the time history of the velocity errors using the velocity controller (28) and (29), which considers viscous and Coulomb friction compensation. Also, Fig. 9 depicts the velocity error using the Dahl-based velocity controller (17)–(19). With controller (28) and (29), the maximum peak error is 9.6° 1/s and 17.3° 1/s for $\tilde{\omega}_1$, and $\tilde{\omega}_2$, respectively, while using the Dahl-based controller (17)–(19) the maximum peak error was 5.92° 1/s and 11.33° 1/s for $\tilde{\omega}_1$, and $\tilde{\omega}_2$, respectively. With respect to the viscous and Coulomb friction compensation controller

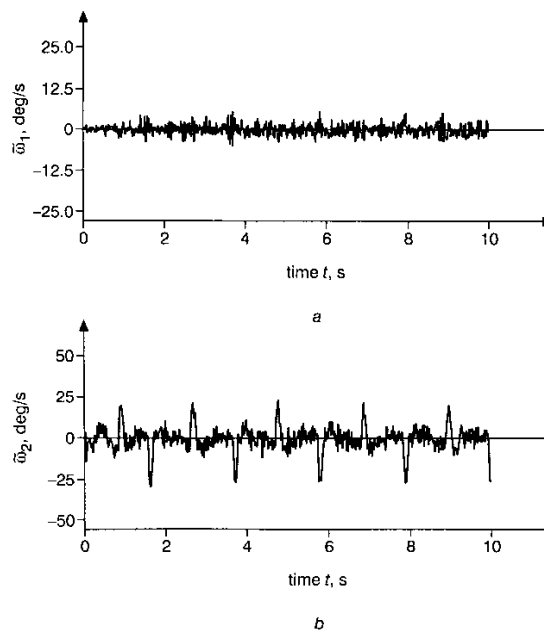


Fig. 7 Velocity error: inverse dynamics with Dahl-based friction compensation (5)–(8)

a $\tilde{\omega}_1$ against time
b $\tilde{\omega}_2$ against time

(28)–(29), the Dahl-based controller (17)–(19) has a better performance. The percentage improvement is 38.33% for $\tilde{\omega}_1$, and 34.51% for $\tilde{\omega}_2$.

4.3 Discussions

The time evolution of the velocity error $\tilde{\omega}$ reflects how well the control system performs. The performance criterion

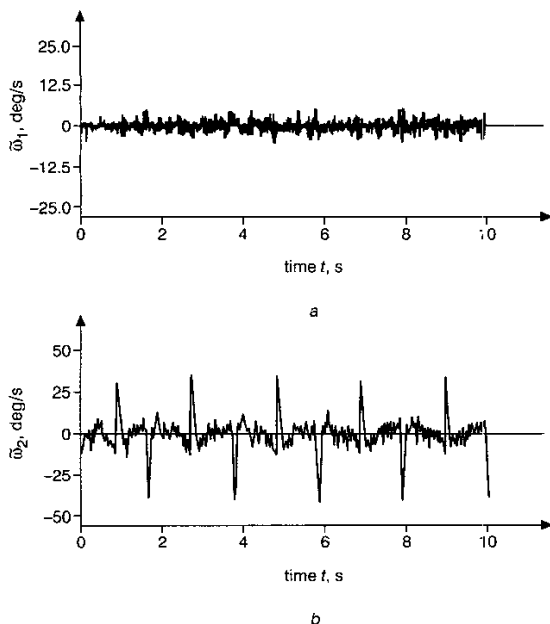


Fig. 6 Velocity error: inverse dynamics with viscous and Coulomb friction compensation (26) and (27)

a $\tilde{\omega}_1$ against time
b $\tilde{\omega}_2$ against time

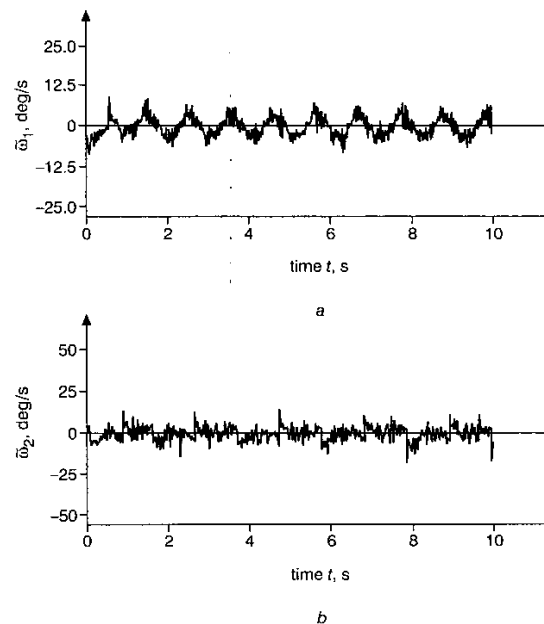


Fig. 8 Velocity error: PD with compensation with viscous and Coulomb friction compensation (28)–(29)

a $\tilde{\omega}_1$ against time
b $\tilde{\omega}_2$ against time

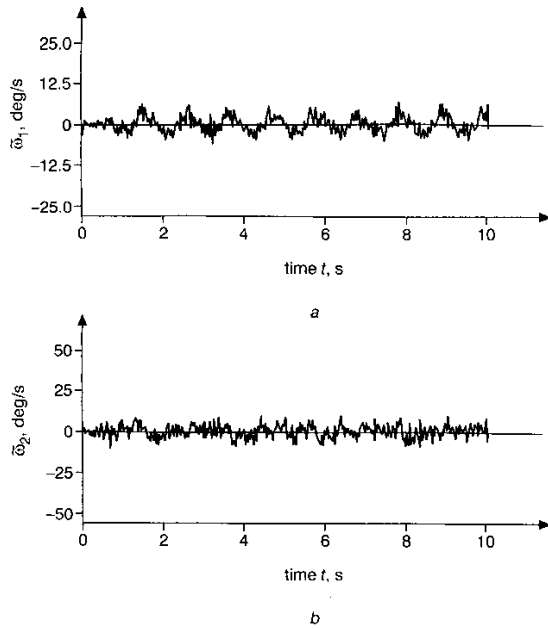


Fig. 9 Velocity error: PD with compensation with Dahl-based friction compensation (17)–(19)

a $\hat{\omega}_1$ against time
b $\hat{\omega}_2$ against time

considered is the root mean square (RMS) value of the velocity error truncated Euclidean norm on a trip of time T , that is:

$$\mathcal{L}_T^2[\tilde{\omega}] = \sqrt{\frac{1}{T} \int_0^T \|\tilde{\omega}(\sigma)\|^2 d\sigma} \quad (\text{rad/s}) \quad (30)$$

The \mathcal{L}_T^2 norm has been previously evoked by several authors as a criterion for tracking performance [18, 19]. In practice, the discrete implementation of the criterion (30) leads to:

$$\mathcal{L}_T^2[\tilde{\omega}] = \sqrt{\frac{1}{T} \sum_{k=0}^i \|\tilde{\omega}(kh)\|^2 h} \quad (\text{rad/s})$$

where $h = 1$ ms is the sampling period and $T = 10$ s is the trip time.

Fig. 10 sketches a bar chart of the values of $\mathcal{L}_T^2[\tilde{\omega}]$ norm for the four tested controllers. With respect to the inverse-dynamics-based controllers, the best performance is

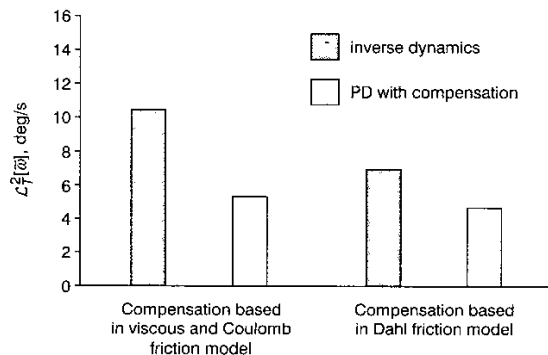


Fig. 10 $\mathcal{L}_T^2[\tilde{\omega}]$ norm

obtained when using Dahl-based friction compensation, i.e. controller (5)–(8), since the $\mathcal{L}_T^2[\tilde{\omega}]$ norm is 27.3% less than the value of the $\mathcal{L}_T^2[\tilde{\omega}]$ norm obtained in the implementation of controller (26) and (27). In implementation of the PD with compensation-based controllers, the best performance is also obtained when using Dahl-based friction compensation, controller (17)–(19). In this case, the norm $\mathcal{L}_T^2[\tilde{\omega}]$ is 11.6% less than the value of the $\mathcal{L}_T^2[\tilde{\omega}]$ norm obtained for controller (28) and (29).

Concerning the experiments of the control structure, the following remarks are in order:

- For the gains used, the norm \mathcal{L}_T^2 is bigger for the inverse-dynamics-based controllers than for the PD with compensation controllers. A better performance can be obtained at the price of exciting high frequency modes of the arm.
- Using the \mathcal{L}_T^2 as a performance index, it is possible to confirm that the use of the Dahl-based friction compensation offers better results in velocity tracking than using classical compensation with a static model of friction. This fact suggests that the Dahl-based observers improve the robustness of the closed-loop system.
- The velocity error peaks are considerably smaller for compensation based on the Dahl model than the peaks observed for control with static friction compensation.

5 Summary

The velocity control in joint space for robot manipulators considering friction at the joints has been addressed. We have proposed two controllers where the friction compensation part is based on the model proposed by Dahl [10]. The experimental results, carried out on a two degrees-of-freedom direct-drive arm, have shown that the proposed controllers have a better performance than those controllers that consider compensation based on the static model of viscous and Coulomb friction.

6 Acknowledgments

This work was partially supported by CONACYT grant 32613-A and SNI, Mexico.

7 References

- 1 ARMSTRONG-HÉLOUVRY, B., DUPONT, P., and CANUDAS DE WIT, C.: 'A survey of analysis tools and compensation methods for the control of machines with friction', *Automatica*, 1994, **30**, (7), pp. 1083–1138
- 2 CANUDAS DE WIT, C., OLSSON, H., ÅSTRÖM, K.J., and LISCHINSKY, P.: 'A new model for control of systems with friction', *IEEE Trans. Autom. Control*, 1995, **40**, (3), pp. 419–425
- 3 CANUDAS DE WIT, C.: 'Comments on A new model for control of systems with friction', *IEEE Trans. Autom. Control*, 1998, **43**, (8), pp. 1189–1190
- 4 DE CARLI, A., CONG, S., and MATACCHIONI, D.: 'Dynamic friction compensation in servodrives'. In Proceedings of the 3rd IEEE conference on Control applications, September 1994, pp. 193–198
- 5 AMIN, J., FRIEDLAND, B., and HARNOY, A.: 'Implementation of a friction estimation and compensation technique', *IEEE Control Syst. Mag.*, 1997, **17**, (4), pp. 71–76
- 6 CANUDAS DE WIT, C., SICILIANO, B., and BASTIN, G. (Eds.): 'Theory of robot control' (Springer-Verlag, London, 1996)
- 7 CORKE, P.: 'The unimation puma servo system'. MTM-226 report, CSIRO Division of Manufacturing Technology, Australia, July 1994
- 8 NILSSON, K.: 'Industrial robot programming'. PhD Dissertation, Dept. of Automatic Control, Lund Institute of Technology, Lund, Sweden, 1996
- 9 LUH, I.Y.S.: 'Conventional controller design for industrial robots—A tutorial', *IEEE Trans. Syst., Man Cybern.*, 1983, **13**, (3), pp. 298–316
- 10 DAHL, P.R.: 'Solid friction damping of mechanical vibrations', *ALAA J.*, 1976, **14**, (12), pp. 1675–1682
- 11 ASADA, H., KANADE, T., and TAKEYAMA, I.: 'Control of a direct-drive arm', *Trans. ASME, J. Dyn. Syst., Meas. Control*, 1983, **105**, pp. 136–142

- 12 BARABANOV, N., and ORTEGA, R.: 'Necessary and sufficient conditions for passivity of the LuGre friction model', *IEEE Trans. Autom. Control*, 2000, **45**, (4), pp. 830-832
- 13 VIDYASAGAR, M.: 'Nonlinear systems analysis' (Prentice Hall, Englewood Cliffs, NJ, 1993)
- 14 SŁOTINE, J., and LI, W.: 'Adaptive manipulator control: a case of study', *IEEE Trans. Autom. Control*, 1988, **33**, (11), pp. 995-1003
- 15 SPONG, M.W., ORTEGA, R., and KELLY, R.: 'Comments on Adaptive manipulator control: a case of study', *IEEE Trans. Autom. Control*, 1990, **35**, (6), pp. 761-762
- 16 KELLY, R., LLAMAS, J., and CAMPA, R.: 'Measurement procedure for viscous and Coulomb friction', *IEEE Trans. Instrum. Meas.*, 2000, **49**, (4), pp. 857-861
- 17 OLSSON, H.: 'Control systems with friction'. PhD Dissertation, Dept. of Automatic Control, Lund Institute of Technology, Lund, Sweden, 1996
- 18 DE JAGER, B., and BANENS, J.: 'Experimental evaluations of robot controllers'. In Proceedings of the 33rd IEEE Conference on Decision and control, Lake Buena Vista, FL, December 1994, pp. 363-368
- 19 JARITZ, A., and SPONG, M.W.: 'An experimental comparison of robust control algorithms on a direct drive manipulator', *IEEE Trans. Control Syst. Technol.*, 1996, **4**, (6), pp. 627-640